Internal report to E89-003 collaboration

Comparison between Kelly and Udias calculations for $^{16}\mathbf{O}(e, e'p)(1p)^{-1}$

James J. Kelly
Department of Physics, University of Maryland,
College Park, MD 20742
Last updated: January 28, 2003

Over the last several years Jose and I have made numerous comparisons between the outputs of our codes using input designed to be as similar as possible. Informal comparisons have generally shown the results to be quite similar, but a more formal comparison is now needed for the PRC paper that Kevin is preparing. This report summarizes the current status of these comparisons, insofar as that information is still available, and should serve as the basis for making the final comparisons needed for the paper. Hopefully we will be able to identify and minimize the sources of any remaining differences over the next couple of weeks. I would like to reduce these differences to the level of numerical noise before undertaking coupled-channels calculations that become extremely time-consuming when Dirac wave functions replace the effective momentum approximation. This is important because both effects are most pronounced at large missing momentum where issues of numerical convergence may arise also. Therefore, please regard this version of the report as work in progress and pardon the inconsistencies in notation and voice produced by splicing text from several sources. Citations of the literature are sporadic and rather incomplete also.

I. MODEL

In this section we present enough of the formalism to outline the calculation in the hopes of identifying significant differences between the two approaches, but omit many of the derivations and most of the steps needed to reduce the formalism to computer code. These details can be filled in later, if necessary.

A. Differential cross section

The fivefold differential cross section for the semi-exclusive $A(e,e'N)B$ reaction leading to a discrete final state takes the form (*eg.* [1])

$$\frac{d^5\sigma}{d\varepsilon_f d\Omega_e d\Omega_N} = K\frac{\varepsilon_f}{\varepsilon_i}\frac{\alpha^2}{Q^4}\eta_{\mu\nu}\mathcal{W}^{\mu\nu} \tag{1}$$

where

$$K = \mathcal{R}\frac{p_N \varepsilon_N}{(2\pi)^3} \tag{2}$$

is a phase-space factor, $k_i = (\varepsilon_i, \mathbf{k}_i)$ and $k_f = (\varepsilon_f, \mathbf{k}_f)$ are the initial and final electron momenta, $p_A = (\varepsilon_A, \mathbf{p}_A)$ and $p_B = (\varepsilon_B, \mathbf{p}_B)$ are the initial and final target momenta, $p_N =$

$(\varepsilon_N, \mathbf{p}_N)$ is the ejectile momentum, $q = k_i - k_f = (\omega, \mathbf{q})$ is the momentum transfer carried by the virtual photon, $Q^2 = -q_\mu q^\mu = \mathbf{q}^2 - \omega^2$ is the photon virtuality, and

$$\mathcal{R} = \left| 1 - \frac{\varepsilon_N}{\varepsilon_B} \frac{\mathbf{p}_N \cdot \mathbf{p}_B}{\mathbf{p}_N \cdot \mathbf{p}_N} \right|^{-1} \tag{3}$$

is a recoil factor which adjusts the nuclear phase space for the constraint on missing energy.

In the one-photon exchange approximation the invariant electroexcitation matrix element is represented by the contraction of electron and nuclear response tensors of the form

$$\eta_{\mu\nu} = \langle j_\mu j_\nu^\dagger \rangle \tag{4}$$

$$W_{\mu\nu} = \langle \mathcal{J}_\mu \mathcal{J}_\nu^\dagger \rangle \tag{5}$$

where j^μ is the electron current, $\mathcal{J}^\mu$ is a matrix element of the nuclear electromagnetic current, and where the angle brackets denote averages over initial and sums over final states to be specified in more detail later. In the present work we assume that the nuclear current is represented by a one-body operator.

B. Electron tensor

In the effective momentum approximation (EMA) for electron distortion, we approximate the electron current by

$$j^\mu(\boldsymbol{q}_{\text{eff}}) \approx \frac{\bar{k}_i \bar{k}_f}{k_i k_f} \bar{u}(\bar{\boldsymbol{k}}_f) \gamma^\mu u(\bar{\boldsymbol{k}}_i) \tag{6}$$

$\boldsymbol{q}_{\text{eff}} = \bar{\boldsymbol{k}}_i - \bar{\boldsymbol{k}}_f$ is the effective momentum transfer based upon the effective wave numbers

$$\bar{\boldsymbol{k}} = \boldsymbol{k} + f_Z \frac{\alpha Z}{R_Z} \hat{\boldsymbol{k}} \tag{7}$$

where $f_Z \approx 1.5$ and $R_Z \approx 1.2 A^{1/3}$. The electron response tensor then takes the form [2]

$$\eta^{\mu\nu} = \frac{1}{2} \left(\eta_0^{\mu\nu} + h \eta_h^{\mu\nu} \right) \tag{8}$$

$$\eta_0^{\mu\nu} = K^\mu K^\nu - q^\mu q^\nu - Q^2 g^{\mu\nu} \tag{9}$$

$$\eta_h^{\mu\nu} = -i \varepsilon^{\mu\nu\alpha\beta} q_\alpha K_\beta \tag{10}$$

where $K^\mu = k_i^\mu + k_f^\mu$ and where K and q are evaluated in the EMA.

C. Nuclear current

In Ref. [3] we developed a formalism for $A(\vec{e}, e'\vec{N})B$ reactions that describes channel coupling in the initial electron $e + A$ wave function as well as in final-state interactions (FSI) of the $N + B$ system. For the present purposes it will be sufficient to summarize the results for channel coupling in FSI neglecting initial-state effects. Let P represent a projection operator for the model space and while $Q = 1 - P$ selects the excluded space.

For single-nucleon knockout we make a parentage expansion of the target ground-state, such that

$$P\psi_0 = \sum_{\beta\gamma} c_{\beta\gamma}\phi_{\beta\gamma}\Phi_\gamma \tag{11}$$

where $c_{\beta\gamma}$ is a parentage coefficient and $\phi_{\beta\gamma}$ is an overlap wave function for removal of a nucleon with single-particle quantum numbers β while leaving the residual nucleus in state Φ_γ. The parentage coefficients $c_{\beta\gamma}$ require two indices whenever the target spin I_0 is nonvanishing. Assuming that the overlap wave functions are described by the Dirac equation, we define upper and lower components by

$$\phi_{\beta\gamma} = \begin{pmatrix} F_{\beta\gamma} \\ i\, G_{\beta\gamma} \end{pmatrix} \tag{12}$$

Similarly, let

$$P\psi_\alpha^{(+)} = \sum_\beta \psi_{\alpha\beta}^{(+)}\Phi_\beta \tag{13}$$

represent an incoming wave function of the $N+B$ system containing an incident plane wave in channel α and outgoing spherical waves in all open channels β for the $B(N,N')B'$ reaction and again employ the Dirac representation to express distorted spinor wave functions as

$$\psi_{\alpha\beta}^{(+)} = \mathcal{N}_\alpha \begin{pmatrix} \chi_{\alpha\beta} \\ i\, \zeta_{\alpha\beta} \end{pmatrix} \tag{14}$$

where

$$\mathcal{N}_\alpha = \sqrt{\frac{E_\alpha + m}{2E_\alpha}} \tag{15}$$

normalizes the asymptotic wave function for channel α to unit flux and where $E_\alpha = \sqrt{k_\alpha^2 + m^2}$ is the channel energy in the barycentric frame. Matrix elements of the current operator for single-nucleon knockout leaving the residual nucleus in asymptotic channel α then take the form

$$\mathcal{J}_\alpha^\mu = \sum_{\beta\gamma} c_{\beta\gamma} \int d^3r\ \exp{(i\boldsymbol{t}\cdot\mathbf{r})}\langle\bar{\psi}_{\alpha\beta}^{(-)}|J_{\text{eff}}^\mu|\phi_{\beta\gamma}\rangle \tag{16}$$

where $\bar{\psi}_{\alpha\beta}^{(-)}$ is the Dirac adjoint of the time-reversed distorted wave and

$$\boldsymbol{t} = \frac{E_B}{W}\mathbf{q} \tag{17}$$

is the recoil-corrected momentum transfer in the barycentric frame. Here $(\omega,\mathbf{q})$ and $E_B = \sqrt{m_B^2 + p_m^2}$ are the momentum transfer and the total energy of the residual nucleus in the laboratory frame and $W = \sqrt{(m_A+\omega)^2 - \mathbf{q}^2}$ is the invariant mass. The effective current operator J_{eff}^μ should include corrections for the excluded space but is usually replaced by the electromagnetic vertex function Γ^μ for a quasifree nucleon.

Working in coordinate space we write

$$\mathcal{J}_{m_0,m_a,m_A}^\mu = \sum_{\beta\gamma m_b m_b'} c_{\beta\gamma} \int d^3r\ \exp{(i\boldsymbol{t}\cdot\mathbf{r})}\langle\bar{\psi}_{\alpha\beta}^{(-)}|\mathbf{r}m_b\rangle\langle\mathbf{r}m_b|\Gamma^\mu|\mathbf{r}m_b'\rangle\langle\mathbf{r}m_b'|\phi_{\beta\gamma}\rangle \tag{18}$$

Matrix elements of the single-nucleon current can be expressed in the block-matrix form

$$\Gamma^{\mu} = \begin{pmatrix} \Gamma^{\mu}_{++} & \Gamma^{\mu}_{+-} \\ \Gamma^{\mu}_{-+} & \Gamma^{\mu}_{--} \end{pmatrix} \tag{19}$$

where each $\langle \mathbf{r} m_b | \Gamma^{\mu}_{\lambda\lambda'} | \mathbf{r} m_b' \rangle$ is a 2×2 matrix in spin while $\lambda = \{+,-\}$ and $\lambda' = \{+,-\}$ partition the upper (+) and lower (-) Dirac components. Note that the dependence upon r allows for the possibility of density-dependent form factors in the vertex function. Let

$$\langle \mathbf{r} m_b' | \phi_{\beta\gamma} \rangle = \begin{pmatrix} F_{\beta\gamma m_b}(\mathbf{r}) \\ i\, G_{\beta\gamma m_b}(\mathbf{r}) \end{pmatrix} \tag{20}$$

represent bound-state overlap wave functions while

$$\langle \bar{\psi}^{(-)}_{\alpha\beta} | \mathbf{r} m_b \rangle = \mathcal{N}_{\alpha} \begin{pmatrix} \chi^{(-)*}_{\alpha\beta m_b}(\mathbf{r}) \\ -i\, \zeta^{(-)*}_{\alpha\beta m_b}(\mathbf{r}) \end{pmatrix} \tag{21}$$

represents the Dirac adjoint of time-reversed distorted waves. The electronuclear matrix elements then take the form

$$\mathcal{J}^{\mu}_{\alpha} = \mathcal{N}_{\alpha} \sum c_{\beta\gamma} \left(\mathcal{J}^{\mu}_{++} + i\mathcal{J}^{\mu}_{+-} - i\mathcal{J}^{\mu}_{-+} + \mathcal{J}^{\mu}_{--} \right) \tag{22}$$

where channel labels are omitted from the $\mathcal{J}^{\mu}_{\lambda\lambda'}$ and where

$$\mathcal{J}^{\mu}_{++} = \int d^3r \; \exp(i\boldsymbol{t}\cdot\mathbf{r}) \chi^{(-)*}_{\alpha\beta m_b}(\mathbf{r}) \Gamma^{\mu}_{++}(m_b, m_b') F_{\beta\gamma m_b'}(\mathbf{r}) \tag{23a}$$

$$\mathcal{J}^{\mu}_{+-} = \int d^3r \; \exp(i\boldsymbol{t}\cdot\mathbf{r}) \chi^{(-)*}_{\alpha\beta m_b}(\mathbf{r}) \Gamma^{\mu}_{+-}(m_b, m_b') G_{\beta\gamma m_b'}(\mathbf{r}) \tag{23b}$$

$$\mathcal{J}^{\mu}_{-+} = \int d^3r \; \exp(i\boldsymbol{t}\cdot\mathbf{r}) \zeta^{(-)*}_{\alpha\beta m_b}(\mathbf{r}) \Gamma^{\mu}_{-+}(m_b, m_b') F_{\beta\gamma m_b'}(\mathbf{r}) \tag{23c}$$

$$\mathcal{J}^{\mu}_{--} = \int d^3r \; \exp(i\boldsymbol{t}\cdot\mathbf{r}) \zeta^{(-)*}_{\alpha\beta m_b}(\mathbf{r}) \Gamma^{\mu}_{--}(m_b, m_b') G_{\beta\gamma m_b'}(\mathbf{r}) \tag{23d}$$

In previous applications of this model final-state interactions were evaluated using a relativized Schrödinger equation for upper components of Dirac wave functions together with an effective momentum approximation (EMA) for the current operator. For simplicity consider a single-channel Dirac equation of the form

$$\left[\boldsymbol{\alpha}\cdot\boldsymbol{p} + \beta(m+S)\right]\psi = (E-V)\psi \tag{24}$$

where

$$\psi(\mathbf{r}) = \begin{pmatrix} \psi_+(\mathbf{r}) \\ \psi_-(\mathbf{r}) \end{pmatrix}$$

is a four-component Dirac spinor. It is well known that the upper component

$$\psi_+ = D^{1/2}\xi \tag{25a}$$

$$D = 1 + \frac{S-V}{E+m} \tag{25b}$$

can be obtained from an equivalent Schrödinger equation of the form

$$\left[\nabla^2 + k^2 - 2\mu\left(U^C + U^{LS}\boldsymbol{L}\cdot\boldsymbol{\sigma}\right)\right]\xi = 0 \tag{26}$$

where k is the relativistic wave number, μ is the reduced energy, and

$$U^C = \frac{E}{\mu}\left[V + \frac{m}{E} + \frac{S^2 - V^2}{2E}\right] + U^D \tag{27a}$$

$$U^D = \frac{1}{2\mu}\left[-\frac{1}{2r^2 D}\frac{d}{dr}(r^2 D') + \frac{3}{4}\left(\frac{D'}{D}\right)^2\right] \tag{27b}$$

$$U^{LS} = -\frac{1}{2\mu}\frac{D'}{rD}\,. \tag{27c}$$

$D(r)$ is known as the Darwin nonlocality factor, and U^C and U^{LS} are central and spin-orbit potentials; the Darwin potential U^D is generally quite small. The lower component is then obtained using

$$\psi_- = \frac{\boldsymbol{\sigma}\cdot\mathbf{p}}{E + m + S - V}\psi_+ \tag{28}$$

Thus, for a single channel the distorted waves can be obtained using the equivalent Schrödinger representation without introducing any new approximation beyond that inherent in describing nucleon-nucleus dynamics by the Dirac equation.

However, such a simple relationship is not available for coupled channels. Although one could, in principle, obtain both upper and lower distorted waves for all channels in the model space by solving the complete system of coupled Dirac equations, models of the structure of excited states and the coupling potentials between them have not been developed as thoroughly within the Dirac framework as in the relativized Schrödinger approach. Furthermore, the system of equations would have much larger dimensionality and it could be very difficult to control the precision of the small components. Therefore, for the purposes of exploratory calculations we assume in this work that the same simple relationship continues to apply in the coupled-channels environment, such that

$$G_{\beta\gamma}(\mathbf{r}) \approx \frac{\boldsymbol{\sigma}\cdot\mathbf{p}}{E_\gamma + m + S_\gamma - V_\gamma}F_{\beta\gamma}(\mathbf{r}) \tag{29a}$$

$$\zeta^{(+)}_{\alpha\beta}(\mathbf{r}) \approx \frac{\boldsymbol{\sigma}\cdot\mathbf{p}}{E_\beta + m + S_\beta - V_\beta}\chi^{(+)}_{\alpha\beta}(\mathbf{r}) \tag{29b}$$

while the upper components are obtained using the relativized Schrödinger model presented in Ref. [4]. In the absence of channel coupling this approach reduces to the familiar relativistic distorted wave approximation for which spinor distortion has been shown to be important to its good description of cross section and recoil polarization data for strong states. The present prescription preserves the spinor distortion for direct knockout while extending the approach to indirect excitation or to large momenta where our earlier investigations indicated that channel coupling becomes important also.

Our previous results using the effective momentum approximation are recovered by replacing the momentum operator in Eq. (29) by the asymptotic momentum for the ejectile or by the missing momentum for the initial state, but in the present application we employ the gradient operator $\mathbf{p} = -i\nabla$. The code also include options for nullifying Dirac scalar and vector potentials for the purpose of investigating the importance of spinor distortion.

D. Partial-wave expansions

We can now express the partial-wave expansion for bound-state overlap wave functions as

$$F_{\beta\gamma m_b}(\mathbf{r}) = F_{\beta\gamma}(r) \sum_{\nu_\gamma m_B} A_{\gamma m_b} Y_{\ell_\gamma \nu_\gamma}(\hat{r}) \tag{30a}$$

$$G_{\beta\gamma m_b}(\mathbf{r}) = G_{\beta\gamma}(r) \sum_{\nu_\gamma m_B} A'_{\gamma m_b} Y_{\ell'_\gamma \nu_\gamma}(\hat{r}) \tag{30b}$$

with $\ell'_\gamma = 2j_\gamma - \ell_\gamma$. The recoupling coefficient for the upper component is given by

$$A_{\gamma m_b} = \langle \begin{matrix} \ell_\gamma & \frac{1}{2} \\ \nu_\gamma & m_b \end{matrix} | \begin{matrix} j_\gamma \\ m_\gamma \end{matrix} \rangle \langle \begin{matrix} j_\gamma & I_B \\ m_\gamma & m_B \end{matrix} | \begin{matrix} I_0 \\ m_0 \end{matrix} \rangle \tag{31}$$

where the angle brackets denote Clebsch-Gordon coefficients, (I_0, m_0) is the target spin, (I_B, m_B) is the spin of the residual nucleus, and m_b is the ejectile spin projection. The recoupling coefficient A'_γ for the lower component has the same form except that $\ell_\gamma \to \ell'_\gamma$. If we assume that these wave functions satisfy standard Dirac equations with spherical scalar and vector potentials, the upper and lower radial wave functions are related by

$$G_{\beta\gamma}(r) = (E_\gamma + m + S_\gamma(r) - V_\gamma(r))^{-1} \left(\frac{\partial}{\partial r} + \frac{\kappa_\gamma + 1}{r} \right) F_{\beta\gamma}(r) \tag{32}$$

where $j_\gamma = |\kappa_\gamma| - \frac{1}{2}$. The radial wave functions are normalized so that

$$\int dr\; r^2 (|F_{\beta\gamma}(r)|^2 + |G_{\beta\gamma}(r)|^2) = 1 \tag{33}$$

It is useful to define the missing momentum distribution as

$$\tilde{F}_{\beta\gamma}(p_m) = \int dr\; r^2 j_{\ell_\gamma}(p_m r) F_{\beta\gamma}(r) \tag{34a}$$

$$\tilde{G}_{\beta\gamma}(p_m) = \int dr\; r^2 j_{\ell'_\gamma}(p_m r) G_{\beta\gamma}(r) \tag{34b}$$

$$S_\beta(p_m) = \frac{4\pi}{(2\pi)^3} \sum_{\gamma\eta} c_{\beta\gamma} c_{\beta\eta} (\tilde{F}_{\beta\gamma}(p_m)\tilde{F}_{\beta\eta}(p_m) + \tilde{G}_{\beta\gamma}(p_m)\tilde{G}_{\beta\eta}(p_m)) \delta_{\ell_\gamma \ell_\eta} \delta_{j_\gamma j_\eta} \tag{34c}$$

where

$$c_{\beta\gamma} \longrightarrow c_\beta \delta_{\beta\gamma} \Longrightarrow S_\beta(p_m) \longrightarrow \frac{|c_\beta|^2}{2\pi^2} \left(|\tilde{F}_\beta(p_m)|^2 + |\tilde{G}_\beta(p_m)|^2 \right) \tag{35}$$

for a single component.

Similarly, the partial-wave expansion for distorted waves with incoming boundary conditions takes the form

$$\chi^{(+)}_{\alpha\beta m_b}(\mathbf{r}) = \frac{4\pi}{k_\alpha r} \sum i^{\ell_\alpha} e^{i\sigma_\alpha} B_{\alpha\beta J} \chi_{\alpha\beta J}(r) Y^*_{\ell_\alpha \nu_\alpha}(\hat{k}_\alpha) Y_{\ell_\beta \nu_\beta}(\hat{r}) \tag{36a}$$

$$\zeta^{(+)}_{\alpha\beta m_b}(\mathbf{r}) = \frac{4\pi}{k_\alpha r} \sum i^{\ell_\alpha} e^{i\sigma_\alpha} B'_{\alpha\beta J} \zeta_{\alpha\beta J}(r) Y^*_{\ell_\alpha \nu_\alpha}(\hat{k}_\alpha) Y_{\ell'_\beta \nu_\beta}(\hat{r}) \tag{36b}$$

where the summations extend over $\{\ell_\alpha \nu_\alpha j_\alpha \ell_\beta \nu_\beta j_\beta J M\}$. The recoupling coefficient for the upper component is given by

$$B_{\alpha\beta J} = \langle {\ell_\alpha \atop \nu_\alpha} {\frac{1}{2} \atop m_a} | {j_\alpha \atop m_\alpha} \rangle \langle {j_\alpha \atop m_\alpha} {I_A \atop m_A} | {J \atop M} \rangle \langle {\ell_\beta \atop \nu_\beta} {\frac{1}{2} \atop m_b} | {j_\beta \atop m_\beta} \rangle \langle {j_\beta \atop m_\beta} {I_B \atop m_B} | {J \atop M} \rangle \tag{37}$$

and the recoupling coefficient $B'_{\alpha\beta J}$ for the lower component is obtained using the replacement $\ell_\beta \to \ell'_\beta = 2j_\beta - \ell_\beta$. The upper components are obtained using a sequential iteration algorithm to solve a relativized Schrödinger equation with coupling potentials obtained by folding density-dependent nucleon-nucleon interactions with local transition densities; details may be found in Ref. [3]. Asymptotically the radial wave functions approach

$$\chi_{\alpha\beta J} \sim \frac{i}{2}\left(\delta_{\alpha\beta} H^*_\beta - S_{\alpha\beta J} H_\beta\right) = \delta_{\alpha\beta} F_\beta + C_{\alpha\beta J} H_\beta \tag{38}$$

where $S_{\alpha\beta J}$ is an element of the S matrix, $C_{\alpha\beta J} = (S_{\alpha\beta J} - \delta_{\alpha\beta})/2i$, and $H_\beta = G_\alpha + iF_\alpha$ is a Coulomb Hankel function with asymptotic form

$$H_\beta \sim \exp\left[i(k_\beta r - \eta_\beta \ln 2k_\beta r - \frac{\ell_\beta \pi}{2} + \sigma_\beta)\right] \tag{39}$$

The Coulomb phase for channel β with ejectile and nuclear charges Z_b and Z_B is given by $\sigma_\beta = \arg\Gamma(\ell_\beta + 1 + i\eta_\beta)$ where $\eta_\beta = Z_b Z_B e^2 \mu_\beta / k_\beta$ is the Sommerfeld parameter. Assuming that the lower component can be approximated using the prescription of Eq. (29), we find

$$\zeta_{\alpha\beta}(r) = \left(E_\beta + m + S_\beta(r) - V_\beta(r)\right)^{-1} \left(\frac{\partial}{\partial r} + \frac{\kappa_\beta}{r}\right) \chi_{\alpha\beta}(r) \tag{40}$$

where $\kappa_\beta = -(\ell_\beta + 1)$ for $j_\beta > \ell_\beta$ or $\kappa_\beta = \ell_\beta$ for $j_\beta < \ell_\beta$.

The time-reversed wave function for the $A(a,b)B$ reaction is obtained via an anti-unitary operator Θ that reverses momenta and spins, such that

$$\psi^{(-)}_{\alpha\beta}(\mathbf{k},\mathbf{r}) = \Theta \psi^{(+)}_{\alpha\beta}(\mathbf{k},\mathbf{r}) = \eta_a \eta_A \eta_{-b} \eta_{-B} \psi^{(+)*}_{-\alpha-\beta}(-\mathbf{k},\mathbf{r}) \tag{41}$$

where negative channel indices indicate reversed spins and where the time-reversal phase for a particle with spin (I_i, m_i) is $\eta_{\pm i} = (-)^{I_i \mp m_i}$. Thus, one can show that the Dirac adjoint for the time-reversed partial-wave expansion takes the form

$$\langle \bar{\psi}^{(-)}_{\alpha\beta} | \mathbf{r} m_b \rangle = \begin{pmatrix} \chi^{(-)*}_{\alpha\beta m_b}(\mathbf{r}) \\ -i\, \zeta^{(-)*}_{\alpha\beta m_b}(\mathbf{r}) \end{pmatrix} \tag{42}$$

where

$$\chi^{(-)*}_{\alpha\beta m_b}(\mathbf{r}) = \frac{4\pi}{k_\alpha r} \sum i^{\ell_\alpha} e^{i\sigma_\alpha} (-)^{2J+\ell_\beta} B_{\alpha\beta J} \chi_{\alpha\beta J}(r) Y_{\ell_\alpha \nu_\alpha}(\hat{k}_\alpha) Y^*_{\ell_\beta \nu_\beta}(\hat{r}) \tag{43a}$$

$$\zeta^{(-)*}_{\alpha\beta m_b}(\mathbf{r}) = \frac{4\pi}{k_\alpha r} \sum i^{\ell_\alpha} e^{i\sigma_\alpha} (-)^{2J+\ell'_\beta} B'_{\alpha\beta J} \zeta_{\alpha\beta J}(r) Y_{\ell_\alpha \nu_\alpha}(\hat{k}_\alpha) Y^*_{\ell'_\beta \nu_\beta}(\hat{r}) \tag{43b}$$

Next we expand the plane wave in the form

$$\exp\left(i\boldsymbol{t} \cdot \mathbf{r}\right) = 4\pi \sum_L i^L j_L(tr) Y_L(\hat{t}) \cdot Y_L(\hat{r}) \tag{44}$$

and choose the $\hat{z}$ axis such that

$$\hat{t} = \hat{z} \Longrightarrow Y_{L\nu}(\hat{t}) Y_{\ell_\alpha \nu_\alpha}(\hat{k}_\alpha) = \frac{\hat{L}}{\sqrt{4\pi}} \delta_{\nu,0} Y_{\ell_\alpha \nu_\alpha}(\theta,\phi) \tag{45}$$

where (θ,ϕ) are the polar and azimuthal angles for the ejectile momentum in the barycentric frame relative to $\bar{t}$. The coordinate-space angular integrals reduce to

$$\int d\hat{r}\; Y^*_{\ell'_\beta \nu_\beta}(\hat{r}) Y_{L\nu}(\hat{r}) Y_{\ell_\gamma \nu_\gamma}(\hat{r}) = (-)^{\nu_\beta} \frac{\hat{\ell}_\beta \hat{L} \hat{\ell}_\gamma}{\sqrt{4\pi}} \begin{pmatrix} \ell_\beta & L & \ell_\gamma \\ 0 & 0 & 0 \end{pmatrix} \begin{pmatrix} \ell_\beta & L & \ell_\gamma \\ -\nu_\beta & 0 & \nu_\gamma \end{pmatrix} \tag{46}$$

where $\ell_\beta \to \ell'_\beta$ for lower components of the ejectile wave and/or $\ell_\gamma \to \ell'_\gamma$ for lower components of the bound-state wave function. The parenthesized arrays denote $3j$ symbols and for angular momenta $\hat{j} = \sqrt{2j+1}$.

Combining these factors, the matrix elements take the form

$$\mathcal{J}^\mu_{\alpha m_0 m_a m_A} = \frac{4\pi}{k_\alpha} \mathcal{N}_\alpha \sum c_{\beta\gamma} i^{\ell_\alpha + L} e^{i\sigma_\alpha} (-)^{2J+\ell_\beta} Y_{\ell_\alpha \nu_\alpha}(\theta,\phi) \left(\tilde{\mathcal{J}}^\mu_{++} + i\tilde{\mathcal{J}}^\mu_{+-} + i\tilde{\mathcal{J}}^\mu_{-+} - \tilde{\mathcal{J}}^\mu_{--} \right) \tag{47}$$

where the summation spans $\{\ell_\alpha j_\alpha \ell_\beta j_\beta L J m_b m'_b \nu_\alpha\}$ but these dependencies of $\tilde{\mathcal{J}}^\mu_{\lambda\lambda'}$ are suppressed to simplify the notation. The coefficients include the sign change resulting from $\ell'_\beta = \ell_\beta \pm 1$ and the effect of γ^0 on $\bar{\psi}$. The four terms

$$\tilde{\mathcal{J}}^\mu_{\lambda\lambda'} = \Upsilon_{\lambda\lambda'} I^\mu_{\lambda\lambda'} \tag{48}$$

are products of overlap integrals of the form

$$\begin{aligned} I^\mu_{++}(m_b m'_b) &= \int dr\; r j_L(tr) \chi_{\alpha\beta J}(r) \Gamma^\mu_{++}(r, m_b, m'_b) F_{\beta\gamma}(r) && \text{(49a)} \\ I^\mu_{+-}(m_b m'_b) &= \int dr\; r j_L(tr) \chi_{\alpha\beta J}(r) \Gamma^\mu_{+-}(r, m_b, m'_b) G_{\beta\gamma}(r) && \text{(49b)} \\ I^\mu_{-+}(m_b m'_b) &= \int dr\; r j_L(tr) \zeta_{\alpha\beta J}(r) \Gamma^\mu_{-+}(r, m_b, m'_b) F_{\beta\gamma}(r) && \text{(49c)} \\ I^\mu_{--}(m_b m'_b) &= \int dr\; r j_L(tr) \zeta_{\alpha\beta J}(r) \Gamma^\mu_{--}(r, m_b, m'_b) G_{\beta\gamma}(r) && \text{(49d)} \end{aligned}$$

and recoupling coefficients of the form

$$\begin{aligned} \Upsilon_{++} &= \Upsilon(m_0 m_a m_A m_b m'_b \nu_\alpha; \ell_\alpha j_\alpha \ell_\beta j_\beta \ell_\gamma j_\gamma L J) && \text{(50a)} \\ \Upsilon_{+-} &= \Upsilon(m_0 m_a m_A m_b m'_b \nu_\alpha; \ell_\alpha j_\alpha \ell_\beta j_\beta \ell'_\gamma j_\gamma L J) && \text{(50b)} \\ \Upsilon_{-+} &= \Upsilon(m_0 m_a m_A m_b m'_b \nu_\alpha; \ell_\alpha j_\alpha \ell'_\beta j_\beta \ell_\gamma j_\gamma L J) && \text{(50c)} \\ \Upsilon_{--} &= \Upsilon(m_0 m_a m_A m_b m'_b \nu_\alpha; \ell_\alpha j_\alpha \ell'_\beta j_\beta \ell'_\gamma j_\gamma L J) && \text{(50d)} \end{aligned}$$

where

$$\begin{aligned} \Upsilon = (2L+1)\hat{\ell}_\beta \hat{\ell}_\gamma \; \sum_{\nu_\gamma} \; (-)^{\nu_\beta} \begin{pmatrix} \ell_\beta & L & \ell_\gamma \\ 0 & 0 & 0 \end{pmatrix} \begin{pmatrix} \ell_\beta & L & \ell_\gamma \\ -\nu_\beta & 0 & \nu_\gamma \end{pmatrix} \left\langle \begin{matrix} \ell_\gamma & \frac{1}{2} \\ \nu_\gamma & m'_b \end{matrix} \middle| \begin{matrix} j_\gamma \\ m_\gamma \end{matrix} \right\rangle \left\langle \begin{matrix} j_\gamma & I_B \\ m_\gamma & m_B \end{matrix} \middle| \begin{matrix} I_0 \\ m_0 \end{matrix} \right\rangle \\ \left\langle \begin{matrix} \ell_\alpha & \frac{1}{2} \\ \nu_\alpha & m_a \end{matrix} \middle| \begin{matrix} j_\alpha \\ m_\alpha \end{matrix} \right\rangle \left\langle \begin{matrix} j_\alpha & I_A \\ m_\alpha & m_A \end{matrix} \middle| \begin{matrix} J \\ M \end{matrix} \right\rangle \left\langle \begin{matrix} \ell_\beta & \frac{1}{2} \\ \nu_\beta & m_b \end{matrix} \middle| \begin{matrix} j_\beta \\ m_\beta \end{matrix} \right\rangle \left\langle \begin{matrix} j_\beta & I_B \\ m_\beta & m_B \end{matrix} \middle| \begin{matrix} J \\ M \end{matrix} \right\rangle \end{aligned} \tag{51}$$

may be formally summed over all remaining spin projections, but only one index remains independent after satisfying the selection rules.

The basic model is now complete. The usual single-channel distorted-wave approximation is recovered by neglecting FSI coupling potentials (other than optical potentials), such that $\chi_{\alpha\beta} \to \chi_\alpha \delta_{\alpha\beta}$, and assuming that the overlap function is well approximated by a unique single-particle wave function, such that $c_{\beta\gamma} \to \delta_{\beta\gamma}\sqrt{(2\ell_\gamma+1)S_\gamma}$ where S_γ is the spectroscropic factor. Similarly, the effective momentum approximation is obtained by replacing the momentum operator in Eq. (29) by the asymptotic momentum and the noSV approximation described in Ref. [4] is obtained by also neglecting Dirac scalar and vector potentials in the construction of lower components of bound and distorted spinors. These approximations provide simpler formulas and faster computations, but the `LEA` program employs the more general formulas presented here.

E. RPWIA

It is frequently useful to employ simpler PWIA calculations to test the partial-wave expansions for DWIA calculations with final-state interactions nullified. Free Dirac spinors take the form

$$u(\mathbf{p},s) = \sqrt{\frac{E+m}{2m}} \begin{pmatrix} 1 \\ \frac{\boldsymbol{\sigma}\cdot\boldsymbol{p}}{E+m} \end{pmatrix} \chi_s \tag{52}$$

for positive energy or

$$v(\mathbf{p},s) = \sqrt{\frac{E+m}{2m}} \begin{pmatrix} \frac{\boldsymbol{\sigma}\cdot\boldsymbol{p}}{E+m} \\ 1 \end{pmatrix} \chi_s \tag{53}$$

for negative energy, where χ_s is a two-component Pauli spinor, and satisfy the orthonormality relations

$$\bar{u}(\mathbf{p},s)\cdot u(\mathbf{p},s') = \delta_{s,s'} \tag{54}$$

$$\bar{v}(\mathbf{p},s)\cdot v(\mathbf{p},s') = \delta_{s,s'} \tag{55}$$

$$\bar{u}(\mathbf{p},s)\cdot v(\mathbf{p},s') = 0 \tag{56}$$

where here the dot product represents contraction with respect to the Dirac index. In the absence of final-state interactions, the ejectile spinor normalized to unit flux becomes

$$\chi_s(\mathbf{p},\mathbf{r}) = \sqrt{\frac{m}{E}} u(\mathbf{p},s) \exp\left(i\mathbf{p}\cdot\mathbf{r}\right) \tag{57}$$

Using the completeness relation

$$\sum_s \left(u_\alpha(\mathbf{p},s)\bar{u}_\beta(\mathbf{p},s) - v_\alpha(\mathbf{p},s)\bar{v}_\beta(\mathbf{p},s)\right) = \delta_{\alpha\beta} \tag{58}$$

matrix elements of the current take the form

$$\mathcal{J}^\mu = \mathcal{J}^\mu_u - \mathcal{J}^\mu_v \tag{59}$$

where

$$\mathcal{J}^{\mu}_{s,u} = \sum_{s'} \bar{u}(\mathbf{p},s)\Gamma^{\mu}u(\mathbf{p},s')\bar{u}(\mathbf{p},s')\cdot\phi_m(\mathbf{p}) \tag{60a}$$

$$\mathcal{J}^{\mu}_{s,v} = \sum_{s'} \bar{v}(\mathbf{p},s)\Gamma^{\mu}v(\mathbf{p},s')\bar{v}(\mathbf{p},s')\cdot\phi_m(\mathbf{p}) \tag{60b}$$

Evaluating the Dirac inner products one finds

$$\bar{u}(\mathbf{p},s')\cdot\phi_m(\mathbf{p}) = i^{-\ell}\sqrt{\frac{E+m}{2m}}\left(\tilde{f}(p) - S_\kappa\frac{p}{E+m}\tilde{g}(p)\right)\mathcal{Y}_{\kappa,m}(\hat{p}) \tag{61a}$$

$$\bar{v}(\mathbf{p},s')\cdot\phi_m(\mathbf{p}) = i^{-\ell}\sqrt{\frac{E+m}{2m}}\left(-\frac{p}{E+m}\tilde{f}(p) + S_\kappa\tilde{g}(p)\right)\mathcal{Y}_{-\kappa,m}(\hat{p}) \tag{61b}$$

where $S_\kappa = \kappa/|\kappa|$ is the sign of κ.

Although the sign of Eq. (61b) differs from Eq. (17) of Caballero *et al.* [5], we are confident in our RPWIA subroutine because it provides good agreement with independent subroutines. Note also that reversal of this sign has severely adverse effects upon recoil polarization.

F. Effective Momentum Approximation

Previous versions of `LEA` employed the effective momentum approximation (EMA) to simplify the evaluation of the nuclear current; this approach is much faster and insight into the role of the spinor distortion can be still be obtained from comparison with this approximation. Assuming that the upper and lower components are related by Eq. (29) using asymptotic kinematics, we approximate the matrix elements of the nuclear expressed by Eq. (18) using

$$\mathcal{J}^{\mu}_{m_0,m_a,m_A} \approx \sum_{\beta\gamma m_b m_b'} c_{\beta\gamma}\int d^3r\ \exp\left(i\boldsymbol{t}\cdot\mathbf{r}\right)\langle\bar{\chi}^{(-)}_{\alpha\beta}|\mathbf{r}m_b\rangle\langle\mathbf{r}m_b|\Gamma^{\mu}_{\mathrm{EMA}}|\mathbf{r}m_b'\rangle\langle\mathbf{r}m_b'|F_{\beta\gamma}\rangle \tag{62}$$

where the EMA current

$$\Gamma^{\mu}_{\mathrm{EMA}} = \tilde{\Lambda}_\alpha(\mathbf{p}_\alpha,r)\gamma^0\Gamma^{\mu}\Lambda_\gamma(\mathbf{p}_\gamma,r) \tag{63}$$

is a 2×2 operator upon Pauli spinors obtained by contraction of the 4×4 Dirac operator $\gamma^0\Gamma^{\mu}$ with 4×2 spinor-distortion operators of the form

$$\Lambda_n(\mathbf{p},r) = \sqrt{\frac{E_n+m}{2m}}\begin{pmatrix} 1 \\ \frac{\boldsymbol{\sigma}\cdot\boldsymbol{p}_n}{E_n+m+S_n(r)-V_n(r)}\end{pmatrix} D_n^{1/2}(r) \tag{64}$$

with the index n distinguishing between the kinematics and potentials appropriate to either the initial or final channels. The partial-wave analysis is similar to that of Sec. I D except that only the upper component of the ejectile and bound spinors are required, reducing the number of overlap integrals by a factor of 4. We identify $\mathbf{p}_\alpha$ with the ejectile momentum and compute the initial momentum $\mathbf{p}_\gamma = \mathbf{p}_\alpha - \mathbf{q}_{\mathrm{eff}}$ using the effective momentum tranfer in the laboratory frame. The energy of the struck nucleon is usually placed on shell by modifying the energy transfer according to the de Forest prescription.

G. Vertex Functions

The electromagnetic vertex function for a free nucleon can be represented by any of three operators [6, 7].

$$\Gamma_1^\mu = \gamma^\mu G_M(Q^2) - \frac{P^\mu}{2M} F_2(Q^2) \tag{65a}$$

$$\Gamma_2^\mu = \gamma^\mu F_1(Q^2) + i\sigma^{\mu\nu}\frac{q_\nu}{2M} F_2(Q^2) \tag{65b}$$

$$\Gamma_3^\mu = \frac{P^\mu}{2M} F_1(Q^2) + i\sigma^{\mu\nu}\frac{q_\nu}{2M} G_M(Q^2) \tag{65c}$$

which are related by the Gordon identity. Here $q = (\omega, \mathbf{q})$, $P = (E' + E, \mathbf{p}' + \mathbf{p})$, and $Q^2 = \mathbf{q}^2 - \omega^2$. Although Γ_2 is arguably the most fundamental because it is defined in terms of the Dirac and Pauli form factors F_1 and F_2, one often uses Γ_1 because its matrix elements are simpler to evaluate. The third form is rarely used but is also equivalent on shell and, hence, is no less fundamental.

Unfortunately, because bound nucleons are not on shell, we require an off-shell extrapolation for which no rigorous justification exists. Lacking a better alternative, we employ the de Forest prescription [6] in which the energies of both initial and final nucleons are placed on shell, based upon effective momenta, and the energy transfer is replaced by the difference between on-shell nucleon energies in the operator but the form factors are still evaluates at the Q^2 from the electron-scattering kinematics. Although most people use this procedure (including Udias, I believe), I am not aware of a strong argument justifying the apparent inconsistency between $\bar{\omega}$ and Q^2. Nevertheless, proceeding in blissful ignorance we obtain the three Gordon-equivalent prescriptions

$$\bar{\Gamma}_1^\mu = \gamma^\mu G_M(Q^2) - \frac{\bar{P}^\mu}{2M} F_2(Q^2) \tag{66a}$$

$$\bar{\Gamma}_2^\mu = \gamma^\mu F_1(Q^2) + i\sigma^{\mu\nu}\frac{\bar{q}_\nu}{2M} F_2(Q^2) \tag{66b}$$

$$\bar{\Gamma}_3^\mu = \frac{\bar{P}^\mu}{2M} F_1(Q^2) + i\sigma^{\mu\nu}\frac{\bar{q}_\nu}{2M} G_M(Q^2) \tag{66c}$$

where

$$\begin{aligned} \bar{q} &= (E' - \bar{E}, \mathbf{q}) \\ \bar{P} &= (E' + \bar{E}, 2\mathbf{p}' - \mathbf{q}) \end{aligned}$$

and where $\bar{E} = \sqrt{m^2 + (\mathbf{p}' - \mathbf{q})^2}$ is placed on shell based upon the externally observable momenta $\mathbf{p}'$ and $\mathbf{q}$. When electron distortion is included, we interpret the local momentum transfer $\mathbf{q} \longrightarrow \mathbf{q}_{\text{eff}}$ as the effective momentum transfer with Coulomb distortion.

It is important to emphasize that both Udias and I evaluate the momenta in these vertex functions using asymptotic kinematics instead of differential operators. This approach is consistent with the EMA for electron distortion and is probably reasonable at high energies for the ejectile, but is questionable for the struck nucleon. Nevertheless, greater effort is probably not justified before a more reliable treatment of the off-shellness of the initial nucleon is available. However, this procedure also raises the issues of frame dependence.

In principle the contraction $\eta_{\mu\nu}\mathcal{W}^{\mu\nu}$ should be a Lorentz scalar, but approximations may produce undesirable frame dependence. Recognizing that distorted waves are evaluated in the barycentric frame, most of my previous calculations used barycentric kinematics in both Γ^μ and $\eta_{\mu\nu}$. Udias, on the other hand, uses laboratory kinematics for both. The difference between these procedures seems to be small, so I will use laboratory kinematics here also to minimize this potential difference. However, I would prefer to have a more compelling argument for the best choice. `LEA` offers both choices, but the `rpwia` subroutine is restricted to laboratory kinematics.

II. OBSERVABLES FOR NUCLEON ELECTROMAGNETIC KNOCKOUT

The cross section for nucleon knockout can be expressed in the form

$$\frac{d^5\sigma}{d\varepsilon_f d\Omega_e d\Omega_N} = \sigma_0 \left[1 + \boldsymbol{P}\cdot\boldsymbol{\sigma} + h(A + \boldsymbol{P}'\cdot\boldsymbol{\sigma})\right] \tag{67}$$

where ε_i (ε_f) is the initial (final) electron energy, σ_0 is the unpolarized cross section, h is the electron helicity, $\boldsymbol{P}$ is the induced polarization, A is the electron analyzing power, and $\boldsymbol{P}'$ is the polarization transfer coefficient. Thus, the net polarization of the recoil nucleon $\boldsymbol{\Pi}$ has two contributions of the form

$$\boldsymbol{\Pi} = \boldsymbol{P} + h\boldsymbol{P}' \tag{68}$$

where $\mid h \mid\leq 1$ is interpreted as the longitudinal beam polarization. We choose to refer recoil polarization to a polarimeter basis in which

$$\hat{\boldsymbol{y}} = \frac{\boldsymbol{k}_i \otimes \boldsymbol{k}_f}{|\boldsymbol{k}_i \otimes \boldsymbol{k}_f|} \tag{69a}$$

$$\hat{\boldsymbol{x}} = \frac{\hat{\boldsymbol{y}} \otimes \boldsymbol{p}_N}{|\hat{\boldsymbol{y}} \otimes \boldsymbol{p}_N|} \tag{69b}$$

$$\hat{\boldsymbol{z}} = \hat{\boldsymbol{x}} \otimes \hat{\boldsymbol{y}} \tag{69c}$$

where $\mathbf{k}_i$ ($\mathbf{k}_f$) are the initial and final electron momenta and $\mathbf{p}_N$ is the ejectile momentum in the laboratory.

The left-right cross section asymmetry

$$A_{LT}(\theta_{pq}) = \frac{\sigma_0(-\theta_{pq}) - \sigma_0(\theta_{pq})}{\sigma_0(-\theta_{pq}) + \sigma_0(\theta_{pq})} \tag{70}$$

for quasiperpendicular kinematics is particularly sensitive to spinor distortion. For coplanar quasiperpendicular kinematics with $\hat{\boldsymbol{y}}$ upwards, it has become conventional to assign positive missing momentum to ejectile momenta on the large-angle side of $\mathbf{q}$, such that $\theta_{pq} = \theta_p - \theta_q > 0$.

It is also useful to define a reduced cross section

$$\sigma_{\text{red}} = \frac{d^5\sigma}{d\varepsilon_f d\Omega_e d\Omega_N} / K\sigma_{eN} \tag{71}$$

where

$$\sigma_{eN} = \frac{\varepsilon_f}{\varepsilon_i}\frac{\alpha^2}{Q^4}\eta_{\mu\nu}\mathcal{W}^{\mu\nu}_{\rm PWIA} \tag{72}$$

is an elementary cross section for electron scattering from a moving free nucleon that is conventionally defined without phase-space factors. The response tensor is given by

$$W^{\mu\nu}_{\rm PWIA} = \frac{1}{2} Trace J^\mu J^{\nu\dagger} \tag{73}$$

where

$$J^\mu_{s_f,s_i} = \sqrt{\frac{m^2}{E_i E_f}}\bar{u}(\mathbf{p}_f, s_f)\Gamma^\mu u(\mathbf{p}_i, s_i) \tag{74}$$

is the single-nucleon current between free spinors normalized to unit flux. The initial momentum $\mathbf{p}_i = \mathbf{p}_f - \mathbf{q}_{\rm eff}$ is obtained from the final ejectile momentum, $\mathbf{p}_f$, and the effective momenum transfer, $\mathbf{q}$, in the laboratory frame and the initial energy is placed on shell. We usually employ the same vertex function for σ_{eN} as for the DWIA calculation, but this quantity is actually free of Gordon ambiguities.

If the nuclear current is evaluated in the effective momentum approximation and final-state interactions are omitted, the reduced current reduces to the contribution of the upper component of the bound-state wave function to the momentum distribution. With appropriate choices for the step size and $\ell_{\rm max}$ one can easily achieve better 1% accuracy for $p_m < 500$ MeV/c or even larger. More generally the reduced cross section in the absence of FSI remains similar to the momentum distribution up to fairly large p_m even though factorization is not satisfied rigorously when the lower component of the bound spinor is distorted. Furthermore, the reduced cross section is determined primarily by the missing momentum and is much less sensitive to other details of the kinematics than is the differential cross section itself.

III. KINEMATICS

For the purposes of this section it is convenient to adorn cm quantities with an asterisk and to assume that quantities without such a mark are in the lab frame; hopefully there will be no confusion with the same notation for complex conjugation.

The missing energy and momentum are defined by

$$E_m = m_N + m_B - m_A \tag{75a}$$
$$\vec{p}_m = \vec{p}_N - \vec{q} \tag{75b}$$

where m_B includes the excitation energy of the residual nucleus. The invariant mass of the residual $N + B$ system is given by

$$W = (m_N^2 + p^{*2})^{1/2} + (m_B^2 + p^{*2})^{1/2} \tag{76}$$

or

$$\begin{aligned} W^2 &= m_A^2 + 2m_A\omega - Q^2 \\ &= (m_N + m_B)^2 + 2m_B T_0 \end{aligned}$$

where

$$p^* = \left((W^2 - m_N^2 - m_B^2)^2 - (2m_N m_B)^2\right)^{1/2} \tag{77}$$

is the relative momentum and

$$T_0 = \frac{m_A}{m_B}\left(\omega - E_m - \frac{Q^2 + E_m^2}{2m_A}\right) \tag{78}$$

is the relative kinetic energy in the final state or, equivalently, the kinetic energy of the ejectile in the rest frame of the residual nucleus. Even though experimentalists prefer to maintain constant p in the lab, the calculations are more conveniently performed with constant p^* in the cm to avoid recalculating the optical potential and the distorted waves (which depend upon the relative kinetic energy) for every kinematical condition. The latter can be done, of course, but is much more time consuming. Furthermore, coupled-channels calculations require the same invariant mass W for all channels and p_m distributions would become prohibitively expensive if W were to vary with p_m. Therefore, unless explicitly specified otherwise, p_m distributions are evaluated for constant W.

Typically we specify p_m or θ_{pq} is the lab but perform the DWIA calculations in the cm. The boost that connects these frames is given by

$$\beta_0 = \frac{q}{m_0 + \omega} \qquad \gamma_0 = \frac{m_0 + \omega}{W} \tag{79}$$

where m_0 is the target ground-state mass.

The ejectile direction is usually specified by the polar angle θ_{pq} relative to the momentum transfer, $\vec{q}$, and the azimuthal angle ϕ_p relative to the electron-scattering plane. However, it is sometimes useful to employ the horizontal angle, α, relative the beam direction and the vertical angle, β, relative to the scattering plane (assumed to be horizontal). These angles are related by

$$\tan(\theta_q - \alpha) = \tan\theta_{pq}\cos\phi_p \tag{80a}$$

$$\sin\beta = \sin\theta_{pq}\sin\phi_p \tag{80b}$$

where θ_q is the angle of $\vec{q}$ relative to the beam.

IV. PWIA TEST

Comparisons between RPWIA and RDWIA calculations for $^{16}\mathrm{O}(e,e'p)(1p_{1/2})^{-1}$ in both quasiperpendicular and parallel kinematics with $T_0 = 427$ MeV are shown in Fig. 1. The RDWIA calculations use the standard partial-wave expansion with optical and Coulomb potentials nullified and use a very large target mass, $m_A = 16001 m_p$, to minimize recoil corrections and frame ambiguities. The step size is 0.05 fm and 80 partial waves are included. Better than 1% agreement is obtained for quasiperpendicular kinematics over the entire p_m range while somewhat larger discrpancies are seen in parallel kinematics for $p_m > 450$ MeV/c and in the immediate vicinity of $p_m = 0$. The variation of Q^2 with p_m is probably responsible for the small oscillations seen in the cross section ratio for parallel kinematics. Nevertheless, this level of precision is considered quite acceptable. Also note that the RPWIA reduced cross section remains relatively close to the momentum distribution except in the immediate vicinity of the node in the contribution of the upper component; the violation of factorization for RPWIA appears mild. Although not shown at this time, we obtain almost perfect agreement for recoil polarization also.

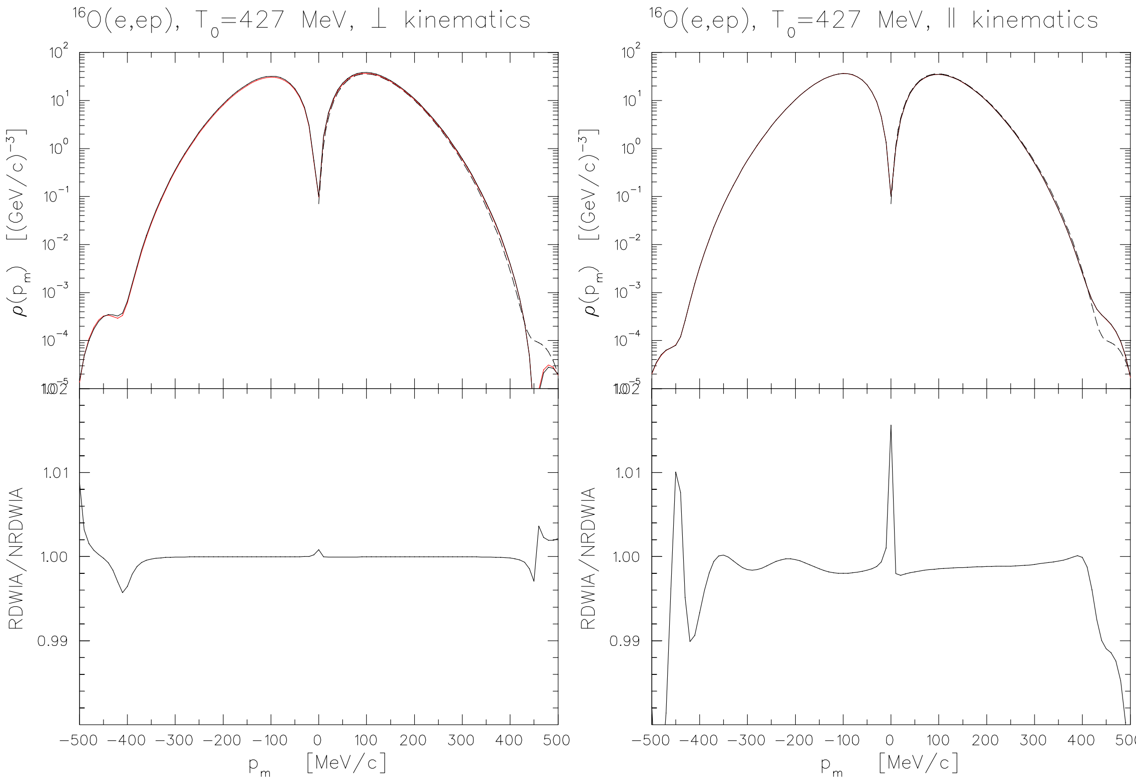

FIG. 1: Comparison between RDWIA and RPWIA calculations for $^{16}\mathrm{O}(e,e'p)(1p_{1/2})^{-1}$ with $T_0 =$ 427 MeV. The upper panels show the reduced RPWIA (black) and RDWIA (red) cross sections and the momentum distribution (dashed). The lower panels show the RDWIA/RPWIA ratio between reduced cross sections.

V. BASELINE CALCULATIONS

The basic DWIA options are listed below. I will add more details about these options and various details of the calculation later, as time permits.

bound-state wave function	NLSH
optical model	EDAIO
nucleon spinor distortion	fully relativistic
electron distortion	none
vertex function	$\bar{\Gamma}_2$
form factors	dipole
gauge	Coulomb

TABLE I: Summary of kinematical conditions.

quantity	$1p_{1/2}$	$1p_{3/2}$	unit	comment
E_0	2441.6	2441.6	MeV	
θ_e	23.204	23.158	deg	
ω	438.617	444.937	MeV	constant
q	991.773	991.773	MeV	constant
Q^2	0.791	0.786	$(\mathrm{GeV}/c)^2$	
θ_q	52.726	52.349	deg	
E_m	12.128	18.448	MeV	
T_0	427.0	427.0	MeV	relative kinetic energy in final state
x_B	0.961	0.941		

Figure 2 compares baseline calculations of the differential cross sections from LEA (solid) and the Madrid code (dashed). There is good overall agreement, but small differences do become apparent for large p_m. Looking closer, Fig. 3 compares ratios between cross section calculations. The solid curves compare my recent calculations using the kinematics listed in Table I with the results provided by Udias on Dec. 6, 2002 that are practically identical to those received in August, 1999. The differences between the two calculations are $\lesssim 2\%$ for $p_m < 250$ MeV/c, but become appreciable for large p_m. The dashed curves comparing my calculations with standard numerical precision options (step size 0.1 fm, 50 partial waves) with more precise calculations (step size 0.05 fm, 80 partial waves) demonstrate convergence over the entire p_m range at the 10^{-3} level using Noumerov integration of the second-order equation. Therefore, the differences between the outputs of the two codes are much larger than the numerical noise in the `LEA` calculation of the nuclear matrix elements.

Despite the increasing differences between the two cross section calculations for $p_m > 300$ MeV/c, Fig. 4 demonstrates that the left-right asymmetry A_{LT} is largely unaffected, showing just a very slight difference in phase. Because this quantity is very sensitive to spinor distortion and details of the current operator, this comparison suggests that these aspects of the two calculations are in very good agreement. Furthermore, it suggests that the cross section differences for $p_m > 300$ MeV/c probably originate in an aspect of the calculation which has little effect upon A_{LT}, such as FSI.

The relatively abrupt deviation between the two cross section calculations for $p_m > 300$ MeV/c appears to be a persistent feature that is very resistant to change. In previous versions there was also a small (2-3%) normalization difference for modest p_m that was probably caused by inconsistency between spinor normalization factors when I evaluated distorted waves in one frame and the current operator in another. That discrepancy has been eliminated. Similarly, in previous versions I used m_B/W instead of E_B/W in Eq. (17), but that effect of that change is almost imperceptible for this range of p_m. The kinematics in the two codes are practically identical and the remaining differences do not appear to affect this comparison either. There was some speculation that small differences in the optical potentials could play a role, but for these calculations I read in the scalar and vector potentials provided by Udias. I suppose that I may still have an error in the construction of the ejectile spinor from the Schrödinger distorted wave, perhaps in the matching to Coulomb functions, but the effect must be subtle and I do not know to test it short of writing an independent routine for solution of the first-order Dirac equation, which would entail yet another validation process.

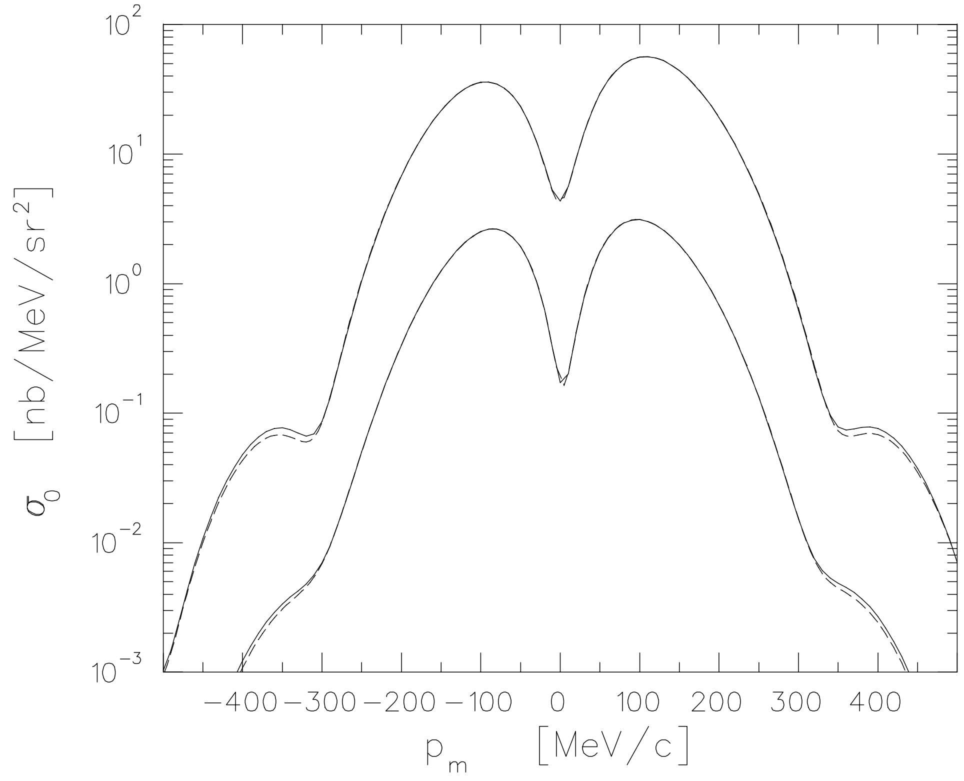

FIG. 2: Baseline LEA (solid) and Madrid (dashed) differential cross sections for $1p$ knockout, normalized to full occupancy. The $1p_{3/2}$ results are multiplied by 10.

[1] J. J. Kelly, Adv. Nucl. Phys. **23**, 75 (1996).
[2] N. Dombey, Rev. Mod. Phys. **41**, 236 (1969).
[3] J. J. Kelly, Phys. Rev. **C 59**, 3256 (1999).
[4] J. J. Kelly, Phys. Rev. **C 60**, 044609 (1999).
[5] J. A. Caballero, T. W. Donnelly, E. M. de Guerro, and J. M. Udías, Nucl. Phys. **A632**, 323 (1998).
[6] T. de Forest, Nucl. Phys. **A392**, 232 (1983).
[7] C. R. Chinn and A. Picklesimer, Il Nuovo Cimento **105A**, 1149 (1992).

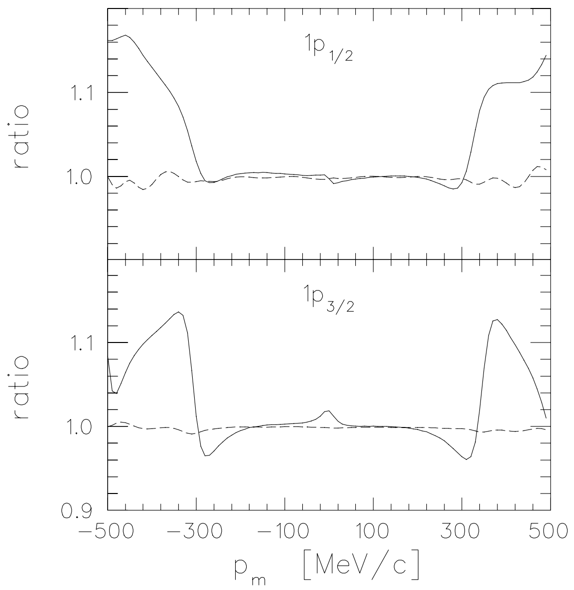

FIG. 3: Ratios between cross section calculations. The dashed lines compare standard and higher precision LEA calculations while the solid lines compare Kelly/Udias.

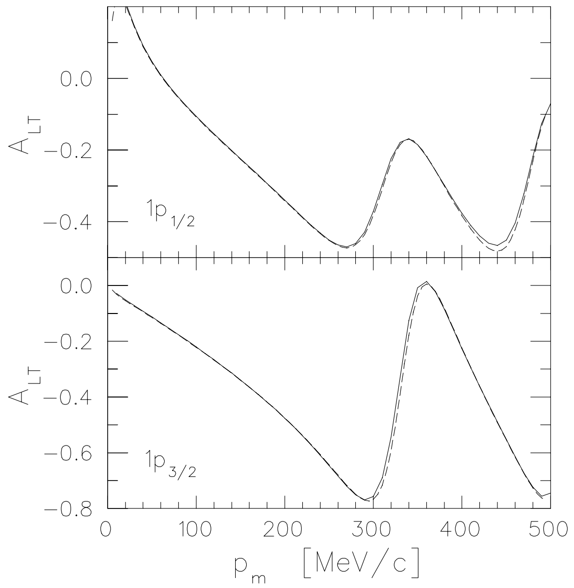

FIG. 4: Solid (dashed) lines show Kelly (Udias) calculations for A_{LT}.